



Published in final edited form as:

Int J Radiat Biol. 2012 March ; 88(3): 213–222. doi:10.3109/09553002.2012.639434.

Accelerated Hematopoietic Toxicity by High Energy ^{56}Fe Radiation

Kamal Datta¹, Shubhankar Suman¹, Daniela Trani¹, Kathryn Doiron¹, Jimmy A. Rotolo², Bhaskar V. S. Kallakury³, Richard Kolesnick⁴, Michael F. Cole⁵, and Albert J. Fornace Jr.^{1,6}

¹Department of Biochemistry and Molecular & Cell Biology and Lombardi Comprehensive Cancer Center, Georgetown University, Room E504 Research Building, 3970 Reservoir Rd., NW, Washington, DC 20057-1468, USA

²Department of Molecular Pharmacology and Chemistry, Memorial Sloan-Kettering Cancer Center, 1275 York Avenue, New York, New York 10021, USA

³Department of Pathology, Georgetown University Medical Center, 119 Basic Science Building, Washington, DC 20057-1468, USA

⁴Laboratory of Signal Transduction, Memorial Sloan-Kettering Cancer Center, 1275 York Avenue, New York, New York 10021, USA

⁵Department of Microbiology and Immunology, Georgetown University Medical Center, Med-Dent SE308A, 3900 Reservoir Road, NW, Washington, DC 20057, USA

⁶Center of Excellence In Genomic Medicine Research (CEGMR), King Abdulaziz University, Jeddah, SA

Abstract

Purpose—There is little information on the relative toxicity of highly charged (Z) high-energy (HZE) radiation in animal models compared to γ or x-rays, and the general assumption based on *in vitro* studies has been that acute toxicity is substantially greater.

Methods—C57BL/6J mice were irradiated with ^{56}Fe ions (1 GeV/nucleon), and acute (within 30 d) toxicity compared to that of γ rays or protons (1 GeV). To assess relative hematopoietic and gastrointestinal toxicity, the effects of ^{56}Fe ions were compared to γ rays using complete blood count (CBC), bone marrow granulocyte-macrophage colony forming unit (GM-CFU), terminal deoxynucleotidyl transferase dUTP nick end labeling (TUNEL) assay for apoptosis in bone marrow, and intestinal crypt survival.

Results—Although onset was more rapid, ^{56}Fe ions were only slightly more toxic than γ rays or protons with lethal dose (LD)_{50/30} (a radiation dose at which 50% lethality occurs at 30-day) values of 5.8, 7.25, and 6.8 Gy respectively with relative biologic effectiveness for ^{56}Fe ions of 1.25 and 1.06 for protons.

Conclusions— ^{56}Fe radiation caused accelerated and more severe hematopoietic toxicity. Early mortality correlated with more profound leukopenia and subsequent sepsis. Results indicate that there is selective enhanced toxicity to bone marrow progenitor cells, which are typically resistant to γ rays, and bone marrow stem cells, because intestinal crypt cells did not show increased HZE toxicity.

*Corresponding author: Albert J. Fornace Jr., M.D., Department of Biochemistry and Molecular & Cell Biology and Lombardi Comprehensive Cancer Center, Georgetown University, Room E504 Research Building, 3970 Reservoir Rd., NW, Washington, DC 20057-1468, USA. Phone: 202 687-7843, Fax: 202 687 3140, af294@georgetown.edu.

Declaration of Interest: The authors report no conflicts of interest.

Keywords

heavy ion radiation; hematopoietic toxicity; myeloid toxicity; gastrointestinal toxicity; space radiation

Introduction

Prolonged missions in outer space will expose astronauts to appreciable cumulative radiation doses with implications for health risks. A major component of space radiation is high-energy protons with relative biological effectiveness (RBE) comparable to γ -radiation for acute lethality and other parameters such as toxicity to intestinal crypt cells (Task Group on the Biological Effects of Space Radiation 1996). In contrast, highly charged (Z) high-energy (HZE) radiation is of particular health concern for astronauts due to its high linear-energy-transfer (high-LET). The high-LET radiation, compared to γ rays and protons, induces very complex repair-refractory DNA damage in cell (Datta et al. 2005, Hada and Sutherland 2006) with implications for survival and genome integrity (Brooks et al. 2001b). One of the most biologically important HZE particles is ^{56}Fe ion. While dose equivalent from proton is only about 5.2%, iron ion contributes almost 22.8% of the galactic cosmic radiation (GCR) dose (Hayatsu et al. 2009). Both primary and secondary delta ray tracks from heavy ion radiation is highly ionizing and will cause significant damage to the cells they traverse (Curtis et al. 1992, Brooks et al. 2001a) with short term as well as long term consequences. Of major short term concern are injury to rapidly proliferating cells in the gastrointestinal (GI) tract and bone marrow (BM), because of the prediction that astronauts could receive enough HZE dose from GCR and solar particle events (SPE) to perturb these tissues in long-term missions (Jakel 2008). Also, in the short term, exposure to ionizing radiation (IR) decreases host immune defense via its effects on the GI tract and BM, thus enhancing the risk of developing local and systemic infection due to endogenous as well as exogenous microorganisms (Brook et al. 2002). Interestingly, apart from changes in intestinal mucosal barrier and defensive barrier of skin, the degree of reduction in the peripheral white blood cell (WBC) count has been directly linked to the risk of systemic infection and mortality (Brook et al. 2004). However, fundamental radiobiological understanding of HZE radiation, its tolerance doses, and its tissue specific toxicity in animal systems is lacking.

In this study, we demonstrate that ^{56}Fe with an RBE of 1.25 was not much more toxic than γ radiation. Furthermore, ^{56}Fe radiation induced early mortality due to accelerated hematopoietic toxicity compared to γ radiation. Finally, we show that profound leukopenia in ^{56}Fe irradiated mice was associated with enhanced bacteremia at the time of their death. These data comparing low- and high-LET radiation effects have important implications not only for safe exploration of space but also for developing optimal strategies for heavy ion radiotherapy (Schulz-Ertner et al. 2006).

Materials and Methods

Mice

Wild type female C57BL/6J mice, 6 to 8 weeks old, were purchased from Jackson Laboratories (Bar Harbor, ME, USA) and were housed 5 mice per cage at the Georgetown University (GU) animal facility which is an Association for Assessment and Accreditation of Laboratory and Animal Care International (AAALACI) accredited facility. All animals (total 348 mice) were housed in a separate room with 12-hour dark and light cycle maintained at 22° C in 50% humidity and certified rodent diet was provided with regular filtered water *ad libitum*. For proton and ^{56}Fe experiments, mice were directly shipped from vendor to Brookhaven National Laboratory (BNL) animal facility, an AAALACI accredited

facility, one week before scheduled exposure. The day after the radiation exposure mice were shipped from BNL in the morning and delivered at GU in the afternoon (same day delivery) in a temperature-controlled environment, which along with direct shipping to BNL was aimed to minimize stress to the animals. Housing conditions at BNL were kept similar to GU. All animal procedures were performed in accordance with a protocol approved by the GU and BNL Institutional Animal Care and Use Committee (IACUC) and Guide for the Care and Use of Laboratory Animals, prepared by the Institute of Laboratory Animal Resources, National Research Council, and U.S. National Academy of Sciences was followed. After receiving from the vendor and before irradiation mice were acclimatized for 1 week at the institutional animal facility. For tissue collection and collection of blood from cardiac puncture, mice were terminally anesthetized using CO₂. For all the irradiated mice efforts were made through daily monitoring to avoid death as an endpoint, but rather a combination of signs (weight loss >15%, reduced activity, hunched posture, and ruffled fur) were used to identify agonal mice and euthanize them.

Radiation

Proton (1 GeV) and ⁵⁶Fe (1 GeV/nucleon) exposures were performed at the National Aeronautics and Space Administration (NASA) Space Radiation Laboratory (NSRL) at Brookhaven National Laboratory (BNL); γ irradiation was done using a ¹³⁷Cs source. Mice (n=10 per group per radiation dose) were irradiated by placing each one in a small transparent rectangular Lucite box (3"×1.5"×1.5") with multiple holes and 10 mice were irradiated at a time. Mice were exposed to 6 to 7.5 Gy of protons, 1 to 8 Gy of ⁵⁶Fe, and 2 to 15 Gy of γ -radiation. The dose rate for all radiation exposures was 1 Gy/min and proton and ⁵⁶Fe exposures at NSRL as well as γ radiation at GU were lateral exposures i.e. beams were horizontal. The proton and ⁵⁶Fe dosimetry was calculated at the NSRL and has been described in detail earlier (Tucker JD et al. 2004, Huang L et al. 2010, Peng Y et al. 2009, Obenaus A et al. 2008). To ensure constant LET values, mice were exposed at the entrance plateau region of the Bragg curve of the beam and beam uniformity ($\pm 2\%$) across the exposure field was calculated by densitometric analysis of exposure images obtained from NSRL Physics laboratory and analyzed using ImageJ v1.45g software. All mice except the 3.5 and 7 day time points mice were monitored for survival for 30 days. For partial body ⁵⁶Fe exposures hind limbs of all the mice (n=10) were shielded with tungsten bricks. Effectiveness of the shielding was determined by measuring the radiation dose behind the shield, which was calculated to be <2% of the total delivered dose. The 30-day survival study after whole body exposure for each radiation type was repeated on 3 different occasions and the partial body experiment was repeated 2 times and representative experiments are shown in figures.

Intestinal histology and crypt microcolony survival assay

Small intestinal tissue samples (n=3 mice per group, per time point, and per radiation dose) were obtained at 3.5 and 7 d after exposure to 10 and 15 Gy of γ radiation and 7 and 8 Gy of ⁵⁶Fe radiation. These doses of γ and ⁵⁶Fe radiation were chosen due to their early mortality rates, which were 100% for all the doses. A small segment of the proximal jejunum was fixed by overnight incubation in 10% neutral buffered formalin and embedded in paraffin blocks. Transverse sections of the tissues were prepared and standard protocol was used to stain all of the sections shown with hematoxylin and eosin (H&E). H&E stained intestinal sections at 3.5 d were also used in the crypt survival assay. The crypt survival assay was performed as described previously (Withers and Elkind 1970, Rotolo et al. 2009). Briefly, the number of surviving crypts defined as containing 10 or more adjacent chromophilic non-Paneth cells, at least one Paneth cell, and a lumen was counted in each cross section. Each cross section served as a unit and six to nine circumferences were scored per mouse, and 3 mice were used to generate each data point. Experiments were repeated

three times, histological images were acquired using bright field microscopy and representative results are shown in figures.

Blood culture

Blood was collected aseptically from mice (n=3 per group, per time point, and per radiation dose) via cardiac puncture in ethylenediaminetetraacetic acid (EDTA) coated tubes at 3.5 and 7 d after exposure to γ (15 Gy) and ^{56}Fe (8 Gy) radiation. Each blood sample (5 μl) was then cultured in triplicate on blood agar plates at 37°C for 48h and bacterial colonies were counted.

Peripheral white blood cell (WBC) count and bone marrow histology

Peripheral WBC counts were performed on samples collected at 3.5, 7, and 28 d post-radiation using a Coulter LH-780 (Beckman Coulter, Brea, CA, USA). Mice (n=3 per group, per time point, and per radiation dose) were irradiated with equitoxic doses of either γ -radiation (2, 2.5, 7.5 or 10 Gy) or ^{56}Fe radiation (respective equitoxic doses are 1.6, 2.0, 6.0 or 8.0 Gy). Blood samples were collected from 3 mice in EDTA tubes. Results are presented as percent of cells per μl of blood. Values are normalized against those from unirradiated control mice. In control mice peripheral white blood cell (WBC) counts (8.01×10^3 per μl of blood, ± 0.81 standard error of mean (SEM)) were within the normal range.

For bone marrow sections (n=3 per group per radiation dose) left femur bone was obtained at 7 d after exposure to γ (2 or 10 Gy) or equitoxic doses of ^{56}Fe (1.6 or 8 Gy) radiation and fixed by overnight incubation in 10% neutral buffered formalin. Decalcified bone marrow was embedded in paraffin blocks and cross sections were H&E stained. Images were captured using bright field microscopy at 40X magnification. A representative area from one section was chosen using fixed pixel (1000 \times 1000) setting in Adobe Photoshop and presented without further reduction in size. These observations were made in three separate experiments and results from one representative experiment are shown in figures.

Granulocyte-Macrophage Colony Forming Unit (GM-CFU) Assay

Colony forming units for granulocyte-macrophage precursor cells were counted as previously described (Pruijt et al. 1999). Mice (n=3 per group per radiation dose) were irradiated either with γ (3.75 or 5 Gy) or equitoxic doses of ^{56}Fe (3 or 4 Gy) radiation. To reduce variability these mice along with the histology, cell cycle, and terminal deoxynucleotidyl transferase dUTP nick end labeling (TUNEL) experiment mice were irradiated on the same day. Bone marrow from the two femurs of each mice was extracted 7 d post-radiation by flushing with Iscove's Modified Dulbecco's Media (IMDM) supplemented with 5% fetal bovine serum (FBS) using a sterile 25G needle. Bone marrow cell suspensions from two femurs of each mouse were pooled and cells were counted with a Coulter counter (Z1; Beckman Coulter) as per manufacturer's instructions. After appropriate dilution of the samples, 2.5×10^4 cells were plated in duplicate in ultra low-attachment 6 well (35 cm) plates (Corning Inc. Corning, NY, USA) with Methocult (M3534; Stem Cell Technologies, Vancouver, BC, Canada) combined with 10 ng/ml murine granulocyte macrophage-colony stimulating factor (GM-CSF; Stem Cell Technologies). Plates were incubated at 37° C in 5% CO₂ and colonies were scored 7 days after incubation using a Leica dissecting scope (MZ6, Leica Microsystems, Wetzlar, Germany).

Cell cycle analysis

Bone marrow cells were collected at 7 d post exposure from control, γ (3.75 Gy), and ^{56}Fe (3 Gy) irradiated mice (n=3 per group per radiation dose) as per protocol described for the GM-CFU assay. Cells were pelleted (200xg for 5 min) at room temperature, supernatant

media was discarded and the cell pellet was washed two times with phosphate buffered saline (PBS). Cells were re-suspended in PBS, fixed in 70% ethanol and kept at -20°C overnight (about 12 hours). Fixed cells were pelleted (400xg for 5 minutes), resuspended in PBS containing 500 $\mu\text{g/ml}$ RNase A (DNase free), and incubated for 45 min at 37°C . After incubation, an equal volume of propidium iodide solution (50 $\mu\text{g/ml}$) in PBS was added and incubated for 15 min at room temperature, and cells were analyzed using FACSCalibur (BD Biosciences, Sparks, MD, USA). Acquired data were analyzed using CellQuest Pro (BD Biosciences). Distribution of cells in G1, S, G2/M, and sub-G1 are presented as percent relative to the total number of events and compared with values in untreated control samples. The sub-G1 peak represents percent of apoptotic/dead cells in a given sample. Both the GM-CFU and cell cycle assays were repeated two times and a representative experiment is shown in the results.

In situ apoptosis detection

Cellular apoptosis in bone marrow sections was examined by the TUNEL method. Mice ($n=3$ per group per radiation dose) were irradiated with 10 Gy of γ -radiation or 8 Gy of ^{56}Fe , sections of 4 μm thickness were cut across the bone marrow after standard fixation, decalcification, and paraffin embedding. Sections were stained using the ApopTag Plus Peroxidase In Situ Apoptosis Detection Kit (Millipore, Billerica, MA, USA) according to the manufacturer's instructions and counterstained with methyl green. Images were acquired using bright field microscopy. Stained sections were quantitated by counting the number of TUNEL positive cells and methyl green stained cells in sections (10 high power fields/section) from 3 separate mice per point and results were presented as average number of positive cells.

Statistics

Lethal dose ($\text{LD}_{50/30}$) (a radiation dose at which 50% lethality occurs at 30-day) was determined by Probit analysis using StatPlus v5.2.0 with 95% confidence interval. All other statistical analyses comparing two different groups were done using two-tailed paired student's t-test and error bar represents \pm standard error of mean (SEM). Statistical analysis of crypt microcolony survival assay was done by one-way analysis of variance (ANOVA) using GraphPad Prism v4. $p<0.05$ was taken as statistically significant.

Results

RBE for ^{56}Fe and proton radiation

The $\text{LD}_{50/30}$ values for γ , proton and ^{56}Fe were determined to be 7.25, 6.8, and 5.8 Gy respectively (Figure 1) with 95% confidence limits of 7.19 and 7.29 for γ , of 6.75 and 6.92 for proton, and of 5.78 and 5.9 for ^{56}Fe radiation. The RBE for proton and ^{56}Fe calculated from this study were respectively, 1.06 and 1.25.

Early lethality after total body ^{56}Fe irradiation

Mice exposed to 15 Gy of γ rays showed early lethality before day 10 post-irradiation, which is typical of GI toxicity. With lower doses (7.5 and 8 Gy) of γ radiation, all the lethality occurred in the second week post-irradiation, but later than day 10, which is typical (Hall and Giaccia 2006) of hematopoietic toxicity (Figure 2A). At a dose of 10 Gy, γ radiation lethality was borderline with all the deaths occurring around day 10 presumably due to some GI toxicity (Hall and Giaccia 2006). With proton radiation all of the lethality occurred in the second week or later (Figure 2B). In contrast, with 6.5, 7 or 8 Gy ^{56}Fe irradiation, all the lethality occurred before 10 days and typically within the first week (Figure 2C). However, when mice were irradiated with their hind limbs shielded and full

doses were delivered to the entire body except the shielded part, all the animals survived for 30 days, even after a dose of 8 Gy of ^{56}Fe (Figure 2D).

HZE and γ radiation induced GI effects

Dose dependent alterations in intestinal crypts and villi in both the γ - and ^{56}Fe -irradiated mice were assessed (Figure 3 and unpublished observations). Exposure to low-LET γ radiation at doses typically above 10 Gy is known to cause lethality within the first week post-exposure due predominantly to GI toxicity, and as the dose increases the contribution of the GI component to mortality also increases (Hall and Giaccia 2006). Histology in the jejunum of mice irradiated with 10 and 15 Gy of γ radiation was compared to 7 and 8 (biologically equivalent to 10 Gy of γ based on an RBE of 1.25) Gy of ^{56}Fe radiation at 3.5 and 7 d post-irradiation (Figure 3A & B). For both time points alterations in crypt and villi structure, like villous shortening, were generally similar between γ and ^{56}Fe radiation, even though rapid lethality was seen at these ^{56}Fe doses (Figure 3A & B). Compared to unirradiated controls, quantization of residual crypts showed significant decreases for both the γ and ^{56}Fe irradiated samples ($p < 0.0001$ for both radiation types). Importantly, we observed a comparable decrease in surviving crypts after exposure to biologically equivalent doses (based on a RBE of 1.25) of γ (10 Gy) and ^{56}Fe (8 Gy) radiation ($p > 0.05$, compare γ and ^{56}Fe radiation) (Figure 3C). Thus, GI injury appears to be similar for γ and ^{56}Fe radiation and indicates a different mechanism for rapid lethality by the latter.

GI-toxicity-mediated lethality after irradiation is due to compromise of the luminal barrier and rapid onset of bacteremia and sepsis. As shown in Figure 3D, there was a pronounced bacteremia 3.5 d after a dose of γ rays that is known to trigger GI toxicity, while there was no significant increase in the bacterial count after the ^{56}Fe dose even though both show early lethality (Figure 2). With profound leukopenia after low LET irradiation, lethality usually occurs at about 2 weeks and is accompanied with septicemia (Hall and Giaccia 2006). Following ^{56}Fe irradiation, septicemia also occurred near the time of death as reflected by a significantly elevated bacterial count at 7 d ($p < 0.004$ compared to 3.5 d count after ^{56}Fe radiation; Figure 3D), even though it was less than that seen for 15 Gy of γ rays where GI lethality clearly occurs.

Differential effects of ^{56}Fe and γ radiation on the hematopoietic system

When peripheral WBC counts in mice irradiated with 2, 7.5 or 10 Gy of γ radiation were compared to counts from ^{56}Fe irradiated (equitoxic doses were 1.6, 6 and 8 Gy respectively), a statistically significant difference was observed. Greater decreases in WBC counts were observed after ^{56}Fe radiation both after 3.5 d ($> 80\%$ reduction at 6 and 8 Gy of ^{56}Fe compared to $< 30\%$ for 7.5 Gy and $< 60\%$ for 10 Gy of γ radiation; $p < 0.004$ for both the doses) (Figure 4A) and at 7 d (just before their death) (77% and 98% reduction at 1.6 and 8 Gy of ^{56}Fe respectively, compared to 68% and 92% reduction at 2 and 10 Gy of γ radiation; $p < 0.01$ for 1.6 Gy & $p < 0.05$ for 8 Gy) (Figure 4B). When the WBC was counted at four weeks post-radiation in surviving mice after γ (2.5 and 7.5 Gy) and equitoxic doses ^{56}Fe radiation (2 and 6 Gy), complete restoration of the counts were observed in animals exposed to 2.5 Gy of γ radiation and partial ($\sim 40\%$) recovery was seen at 7.5 Gy (Figure 4C). In contrast, significantly lower recovery was observed after 2 ($p < 0.002$ compared to 2.5 Gy of γ radiation) and 6 Gy ($p < 0.04$ compared to 7.5 Gy of γ radiation) of ^{56}Fe -irradiated mice at this time (Figure 4C). Examination of H&E stained bone marrow sections from mice exposed to a sub-lethal doses of ^{56}Fe (1.6 Gy) radiation showed a greater reduction in myeloid precursor cells (Figure 4D) compared to γ (2 Gy) radiation, which is consistent with our observations for WBC counts. Myeloid precursors are larger than erythroid precursors and have oval, eccentrically placed nucleus, granular cytoplasm, and diffuse chromatin. Erythroid precursors are smaller than myeloid precursors with round

nucleus filling the cell, and dense and darker chromatin. In order to better characterize the differential effects of these two types of radiation on the hematopoietic system, we compared bone marrow sections from animals exposed to lethal equitoxic doses of γ rays (10 Gy) or ^{56}Fe ions (8 Gy) at 3.5 and 7 d post-irradiation. Although there was a marked decrease in bone marrow cellularity compared to control (Figure 5A) after this γ ray dose, clusters of precursor cells were observed in patches throughout the section (Figure 5B). In contrast, for the same time point, very few scattered precursor cells, but no clusters were observed in samples from ^{56}Fe -exposed animals (Figure 5C). Compared to γ -irradiated samples, a lesser number of myeloid precursors, and mostly erythroid precursors, were observed after ^{56}Fe radiation. Similar, albeit less cellular, patterns were also observed in 7 d post-radiation for both γ (Figure 5E) and ^{56}Fe exposed animals (Figure 5F).

This phenomenon of selective lethality towards myeloid cells by ^{56}Fe radiation was further investigated by bone marrow GM-CFU assay at 7 d after exposure to two sub-lethal doses of γ radiation (3.75 or 5 Gy) and respective equitoxic doses of ^{56}Fe ions (3 and 4 Gy). Compared to the corresponding equitoxic dose of γ rays, we observed significantly fewer colonies for both the 3 Gy ($p < 0.003$) and the 4 Gy ($p < 0.04$) of ^{56}Fe radiation (Figure 6A) supporting our results from WBC counts and bone marrow histology.

Cell cycle analysis showed significant differences in distribution pattern of bone marrow cells harvested at 7 d after exposure to either 3.75 Gy of γ -radiation or 3 Gy of ^{56}Fe radiation. Mice irradiated with ^{56}Fe showed a significant decrease in the G1 population ($p < 0.004$ compared to γ -radiation), and a significant increase in both S ($p < 0.01$ compared to γ radiation) and G2/M populations ($p < 0.04$ compared to γ radiation) (Figure 6B). γ radiation did not show a significant change in the G1 cell population ($p > 0.05$ compared to control) but did show a decrease in the S-phase population ($p < 0.02$ compared to control) and an increase in G2/M-phase ($p < 0.04$ compared to control) cells. Interestingly, cells in G2/M in ^{56}Fe samples were significantly higher ($p < 0.04$ compared to γ radiation) than those in γ irradiated samples. We also observed that compared to equitoxic doses of γ rays, exposure to ^{56}Fe radiation led to a more pronounced increase in the G2/G1 ratio (Figure 6C) and the sub-G1 population (Figure 6D), which respectively indicate G2 arrest and cell death.

TUNEL staining performed on bone marrow sections after 3.5 d showed a markedly higher number of apoptotic cells in ^{56}Fe -irradiated (8 Gy) samples compared to an equitoxic dose of γ rays (10 Gy) (Figure 7A). In contrast, more nuclear stained precursor cells were observed in γ -irradiated mice. Quantification of TUNEL positive and nuclear-stain positive cells showed significant difference between γ and ^{56}Fe radiation exposures ($p < 0.002$ for TUNEL positive count and $p < 0.001$ for nuclear stain positive cells) (Figure 7B).

Discussion

Determining the RBE of various parameters for space radiation in comparison to terrestrial radiation exposures is important for risk assessment. Since there is sufficient statistical sampling for the latter, risk estimates can then be extrapolated to particle radiation using a RBE scaling factor. Current study was initiated to determine the RBE of proton and ^{56}Fe in female C57BL/6J mice so that the RBE factor could be used to calculate doses of proton and ^{56}Fe equitoxic to γ radiation for our intestinal tumorigenesis study in adenomatous polyposis coli (APC) mutant mouse models (Trani et al. 2010), which are also in C57BL/6J background. Typically, radiation carcinogenesis studies are carried out at high sub-lethal doses to maximize tumor yield (Hollander et al. 1999; Trani et al. 2010), and then extended to lower doses where indicated and feasible. Lack of sufficient *in vivo* data in the literature on the relative toxicity of proton and ^{56}Fe radiation in these mice required us to use high doses of these radiation types to obtain $\text{LD}_{50/30}$ and determine the RBE factor in relation to

γ radiation for the ongoing intestinal tumorigenesis study. It should also be noted that mice are substantially more resistant than humans to killing with a γ -ray LD₅₀ nearly twice that for humans (without therapeutic intervention) (Hall and Giaccia 2006). RBE values for protons with energies above 0.05 GeV have been shown to be close to 1 (Gueulette et al. 1997). In our study, consistent with previous reports, the RBE for the LD_{50/30} for 1 GeV protons was 1.06 and showed a similar timeframe for onset of lethality as γ rays. HZE ions such as high-energy ⁵⁶Fe due to their high tissue penetrability are of particular concern during deep space exploration. Considering the high-LET nature and the capability of inducing complex repair-refractory damage, we expected a higher RBE value for ⁵⁶Fe radiation. Indeed, the RBE for cell killing by high-LET radiation, such as α -rays or neutrons, is much more than 1 (Hall and Giaccia 2006), and the HZE RBE for late effects, such as cataractogenesis, can also be quite high (Task Group on the Biological Effects of Space Radiation 1996). However, with an observed RBE of 1.25 for LD_{50/30}, ⁵⁶Fe ions (1 GeV/nucleon; LET- 148 KeV/ μ m) were not much more toxic than γ rays and protons. Previous studies have shown that the RBE for particle radiation as a function of LET is variable and is dependent on the particle's energy (Gueulette et al. 1997). A low RBE for ⁵⁶Fe ions, although surprising, is not unprecedented, and has been reported previously with other high-LET radiation in a variety of cellular and animal studies, such as colony formation of BM cells, testicular weight loss, and life shortening experiments (Ainsworth 1986, George et al. 2003). In these experiments the RBE increased with LET and peaked at an LET of about 100 KeV/ μ m, and then diminished so that RBE values of <2 were observed for LET above 100 KeV/ μ m (Ainsworth 1986, George et al. 2003); and our study's ⁵⁶Fe beam has a LET of 150. Presumably, LET-dependent characteristics of track structure, energy deposition, and distribution pattern of primary and secondary ionization events contribute to varying RBE of various HZE ions (Brooks et al. 2001a).

During the course of our RBE study we were surprised to find that all of the high-LET radiation mortality occurred on or before 7 d post-radiation and coincided with the timeframe for radiation-induced GI syndrome observed after 15 Gy of γ radiation (Komarova et al. 2004, Rotolo et al. 2009). In an effort to understand this phenomenon of early lethality in high-LET irradiated (⁵⁶Fe) mice, we assessed the hematopoietic and GI systems. To this end, when mice were ⁵⁶Fe-irradiated with their hind limbs shielded - protecting in this way some of the bone marrow, but delivering the full dose to the rest of the body - we did not observe any lethality in the 30 days after exposure even at 8 Gy, otherwise a 100% lethal dose after whole body exposure. If whole-body exposed mice were dying predominantly of GI toxicity, shielding of bone marrow would not have altered the observed early lethality pattern. On the contrary, our observation is suggestive of the fact that bone marrow failure rather than the GI syndrome is playing a determining role in the accelerated ⁵⁶Fe lethality in our experimental setting. A tenet of radiobiology is that rapidly proliferating early progenitor cells in the BM, and presumably pluripotent hematopoietic stem cells, are more sensitive to IR than more mature progenitor and differentiated cells, and thus these latter cells need to turnover before profound leukopenia occurs (Hall and Giaccia 2006). An obvious explanation for accelerated mortality observed with ⁵⁶Fe ions is that they are selectively more toxic toward more mature progenitor and differentiated cells. This conclusion is consistent with our observations in peripheral blood and bone marrow at the early post-radiation time point of 3.5 d and also just before the lethality occurred, 7 d. For instance, a lethal dose of 10 Gy of γ -radiation only reduced the WBC count by about half at 3.5 d, while an equitoxic dose of ⁵⁶Fe ions (8 Gy) showed a significantly greater decrease (>80%) at the same post-irradiation time. A similar greater decrease in WBC count (>80%) at 6 Gy ⁵⁶Fe, a dose equitoxic to 7.5 Gy of γ rays for which we observed only <30% decrease, suggests that sensitivity of myeloid cells to high-LET radiation commences even at a lower dose which is only partially lethal. The trend in differential changes for WBC after low- and high-LET radiation was confirmed also at the terminal stage, 7 d, of the

animal. Furthermore, at this time, there was also far more suppression of bone marrow GM-CFU at equitoxic sub-lethal doses of ^{56}Fe ions. We speculate that enhanced mortality with ^{56}Fe could be due to preferential myeloid toxicity with enhanced killing of progenitor cells (in addition to stem cells) that are resistant to γ -radiation killing. Our results are consistent with earlier *in vitro* studies, which showed that bone marrow stem cells as well as myeloid progenitors are more sensitive to high-LET neutron radiation than low-LET γ radiation (Millard and Blackett 1981). When compared between two cell types, BM stem cells showed greater sensitivity to both γ and neutron radiation than myeloprogenitors. However, unlike neutrons, which were uniformly lethal, γ radiation induced a biphasic response in myeloprogenitors with a subset (20–50%) of these cells showing more resistance (Millard and Blackett 1981). Quantization of nucleated BM cells in our TUNEL assay not only reflects a subset of surviving precursor cells after γ radiation but also is in complete agreement with our WBC results; there were far more non-apoptotic nucleated cells after a lethal dose of γ rays, than after ^{56}Fe ions. In contrast, these two types of radiation affected GI epithelium similarly with approximately equivalent crypt survival with equitoxic doses (Figure 3C). Results were strikingly different with 15 Gy of γ rays where mortality is primarily due to GI toxicity where early bacteremia occurred. Considering our results on crypt count, intestinal histology, and bacteremia along with WBC and bone marrow data, we believe early lethality in ^{56}Fe mice is predominantly due to hematopoietic toxicity rather than predominant GI toxicity which was suggestive by the observed mortality timecourse. We propose that early profound leukopenia leading to severe immunosuppression and subsequent infection is the major contributing factor in the early death of ^{56}Fe -exposed mice.

Considering our results for rapid and profound reductions of WBC and nucleated BM cells along with increase in G2/G1 ratio and an increase in sub-G1 population after ^{56}Fe ions, it is reasonable to conclude that 1 GeV/n ^{56}Fe ions exerts preferential toxicity towards the myeloid compartment, and that more mature myeloid bone marrow and lymphoid progenitor cells, which are typically resistant to direct killing by γ rays, are susceptible to heavy ion radiation. Although a number of recent studies tested sensitivity of myeloid cells to high-LET radiation using various parameters (Gridley et al. 2002, Pecaut and Gridley 2010, Gridley and Pecaut 2011), ours is the first report showing *in vivo* differential sensitivity of the hematopoietic system to γ and heavy ion radiation.

Conclusions

Radiosensitivity of hematopoietic cells to the two types of radiation was different with myeloid compartment showing greater sensitivity towards ^{56}Fe than γ radiation. We believe that our findings have implications for development of effective countermeasure strategy against heavy ion radiation toxicity on normal tissues. However, the implications of our observations for space travel associated carcinogenesis remains to be determined. Although beyond the scope of the current study, it will be important to investigate in detail the radiosensitivity of various bone marrow stem cell and progenitor lineages and the molecular pathways that underlie the tissue responses reported here. A better understanding of differential radiosensitivity of specific subpopulations of hematopoietic cell lineages may contribute not only to post-exposure carcinogenic risk estimate but also to safer therapeutic use of heavy ion radiation.

Acknowledgments

This work was supported by NASA Grants (NNX07AH70G and NNX09AU95G). Dr. D. Trani was supported by the National Space Biomedical Research Institute (NSBRI) through NASA NCC9-58. Efforts at Memorial Sloan-Kettering Cancer Center were supported by National Cancer Institute (NCI) RO1-85704. We thank Dr. K. Sree Kumar at Armed Forces Radiobiology Research Institute (AFRRI) for his valuable suggestions. We are also

thankful to Dr. Adam Rusek, Dr. Peter Guida, and the NASA space radiation research laboratory at Brookhaven National Laboratory for their support.

Bibliography

- Ainsworth EJ. Early and late mammalian responses to heavy charged particles. *Advances in Space Research*. 1986; 6:153–165. [PubMed: 11537215]
- Brook I, Elliott TB, Ledney GD, Knudson GB. Management of postirradiation sepsis. *Military Medicine*. 2002; 167:105–106. [PubMed: 11873487]
- Brook I, Elliott TB, Ledney GD, Shoemaker MO, Knudson GB. Management of postirradiation infection: lessons learned from animal models. *Military Medicine*. 2004; 169:194–197. [PubMed: 15080238]
- Brooks A, Bao S, Rithidech K, Couch LA, Braby LA. Relative effectiveness of HZE iron-56 particles for the induction of cytogenetic damage in vivo. *Radiation Research*. 2001a; 155:353–359. [PubMed: 11175671]
- Brooks AL, Bao S, Rithidech K, Chrisler WB, Couch LA, Braby LA. Induction and repair of HZE induced cytogenetic damage. *Physica Medica*. 2001b; 17(Suppl 1):183–184. [PubMed: 11776254]
- Curtis SB, Townsend LW, Wilson JW, Powers-Risius P, Alpen EL, Fry RJ. Fluence-related risk coefficients using the Harderian gland data as an example. *Advances in Space Research*. 1992; 12:407–416. [PubMed: 11537038]
- Datta K, Neumann RD, Winters TA. Characterization of complex apurinic/aprimidinic-site clustering associated with an authentic site-specific radiation-induced DNA double-strand break. *Proceedings of the National Academy of Sciences of the United States of America*. 2005; 102:10569–10574. [PubMed: 16024726]
- George K, Durante M, Willingham V, Wu H, Yang TC, Cucinotta FA. Biological effectiveness of accelerated particles for the induction of chromosome damage measured in metaphase and interphase human lymphocytes. *Radiation Research*. 2003; 160:425–435. [PubMed: 12968931]
- Gridley DS, Pecaat MJ. Genetic background and lymphocyte populations after total-body exposure to iron ion radiation. *International Journal of Radiation Biology*. 2011; 87:8–23. [PubMed: 21067301]
- Gridley DS, Pecaat MJ, Nelson GA. Total-body irradiation with high-LET particles: acute and chronic effects on the immune system. *American Journal of Physiology - Regulatory Integrative and Comparative Physiology*. 2002; 282:R677–88.
- Gueulette J, Bohm L, De Coster BM, Vynckier S, Octave-Prignot M, Schreuder AN, Symons JE, Jones DT, Wambersie A, Scalliet P. RBE variation as a function of depth in the 200-MeV proton beam produced at the National Accelerator Centre in Faure (South Africa). *Radiotherapy and Oncology*. 1997; 42:303–309. [PubMed: 9155083]
- Hada M, Sutherland BM. Spectrum of complex DNA damages depends on the incident radiation. *Radiation Research*. 2006; 165:223–230. [PubMed: 16435920]
- Hall, EJ.; Giaccia, AJ. *Radiobiology for the Radiologist*. Lippincott Williams & Wilkins; Philadelphia: 2006.
- Hayatsu K, Hareyama M, Kobayashi S, Yamashita N, Sakurai K, Hasebe N. HZE Particle and Neutron Dosages from Cosmic Rays on the Lunar Surface. *Journal of the Physical Society of Japan*. 2009; 78:149–152.
- Hollander MC, Sheikh MS, Bulavin DV, Lundgren K, Augeri-Henmueller L, Shehee R, Molinaro TA, Kim KE, Tolosa E, Ashwell JD, Rosenberg MP, Zhan Q, Fernández-Salguero PM, Morgan WF, Deng CX, Fornace AJ Jr. Genomic instability in Gadd45a-deficient mice. *Nature Genetics*. 1999; 23:176–184. [PubMed: 10508513]
- Huang L, Smith A, Badaut J, Obenaus A. Dynamic characteristics of 56Fe-particle radiation-induced alterations in the rat brain: magnetic resonance imaging and histological assessments. *Radiation Research*. 2010; 173:729–737. [PubMed: 20518652]
- Jakel O. The relative biological effectiveness of proton and ion beams. *Journal Medical Physics*. 2008; 18:276–285.

- Komarova EA, Kondratov RV, Wang K, Christov K, Golovkina TV, Goldblum JR, Gudkov AV. Dual effect of p53 on radiation sensitivity in vivo: p53 promotes hematopoietic injury, but protects from gastro-intestinal syndrome in mice. *Oncogene*. 2004; 23:3265–3271. [PubMed: 15064735]
- Millard RE, Blackett NM. Radiosensitivity and recovery of two murine haemopoietic progenitor cell populations following gamma rays and neutrons. *Acta Haematologica*. 1981; 66:226–232. [PubMed: 6800187]
- Obenaus A, Huang L, Smith A, Favre CJ, Nelson G, Kendall E. Magnetic resonance imaging and spectroscopy of the rat hippocampus 1 month after exposure to ⁵⁶Fe-particle radiation. *Radiation Research*. 2008; 169:149–161. [PubMed: 18220468]
- Pecaut MJ, Gridley DS. The impact of mouse strain on iron ion radio-immune response of leukocyte populations. *International Journal of Radiation Biology*. 2010; 86:409–419. [PubMed: 20397846]
- Peng Y, Brown N, Fannon R, Warner CL, Liu X, Genik PC, Callan MA, Ray FA, Borak TB, Badie C, Bouffler SD, Ullrich RL, Bedford JS, Weil MM. Radiation leukemogenesis in mice: loss of PU.1 on chromosome 2 in CBA and C57BL/6 mice after irradiation with 1 GeV/nucleon ⁵⁶Fe ions, X rays or gamma rays. Part I. Experimental observations. *Radiation Research*. 2009; 171:474–483. [PubMed: 19397448]
- Pruijt JF, Fibbe WE, Laterveer L, Pieters RA, Lindley IJ, Paemen L, Masure S, Willemze R, Opendakker G. Prevention of interleukin-8-induced mobilization of hematopoietic progenitor cells in rhesus monkeys by inhibitory antibodies against the metalloproteinase gelatinase B (MMP-9). *Proceedings of the National Academy of Sciences of the United States of America*. 1999; 96:10863–10868. [PubMed: 10485917]
- Task Group on the Biological Effects of Space Radiation, Space Studies Board, Commission on Physical Sciences, Mathematics, and Applications, National Research Council. *National Academy Press*; Washington, DC: 1996. Radiation hazards to crews of interplanetary missions: biases.
- Rotolo JA, Kolesnick R, Fuks Z. Timing of lethality from gastrointestinal syndrome in mice revisited. *International Journal of Radiation Oncology, Biology, Physics*. 2009; 73:6–8.
- Schulz-Ertner D, Jakel O, Schlegel W. Radiation therapy with charged particles. *Seminars in Radiation Oncology*. 2006; 16:249–259. [PubMed: 17010908]
- Trani D, Datta K, Doiron K, Kallakury B, Fornace AJ Jr. Enhanced intestinal tumor multiplicity and grade in vivo after HZE exposure: mouse models for space radiation risk estimates. *Radiation and Environmental Biophysics*. 2010; 49:389–396. [PubMed: 20490531]
- Tucker JD, Marples B, Ramsey MJ, Lutze-Mann LH. Persistence of chromosome aberrations in mice acutely exposed to ⁵⁶Fe+26 ions. *Radiation Research*. 2004; 161:648–655. [PubMed: 15161355]
- Withers HR, Elkind MM. Microcolony survival assay for cells of mouse intestinal mucosa exposed to radiation. *International Journal of Radiation Biology & Related Studies in Physics Chemistry & Medicine*. 1970; 17:261–267.

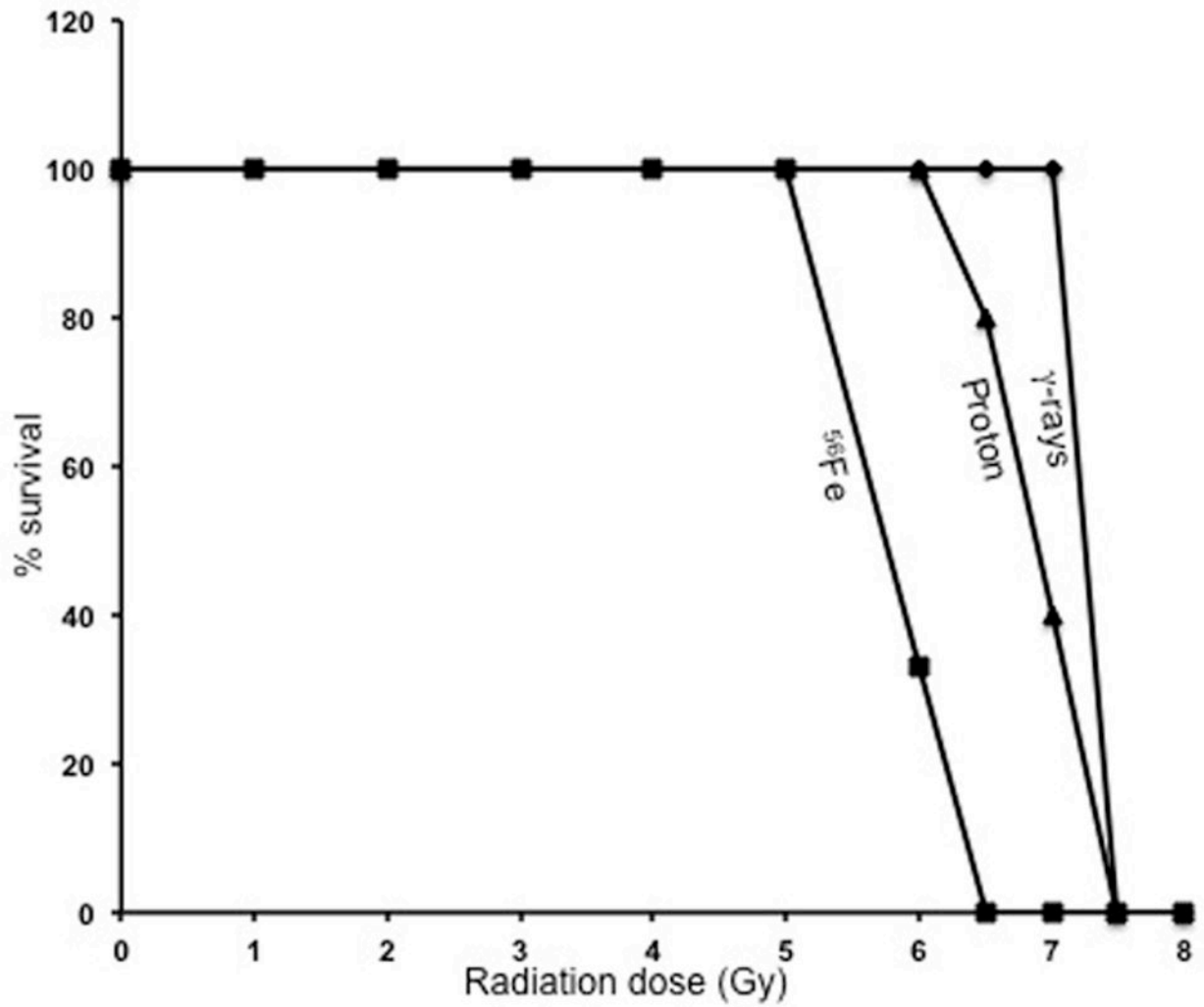


Figure 1.

In vivo lethality was determined for ^{56}Fe -, proton-, and γ -radiation. Mice (n=10 per group per radiation dose) were irradiated with the ^{56}Fe ions (1 to 8 Gy), protons (6 to 7.5 Gy), and γ rays (5 to 8.5 Gy), and survival was monitored for 30 days; results are plotted as percent survival.

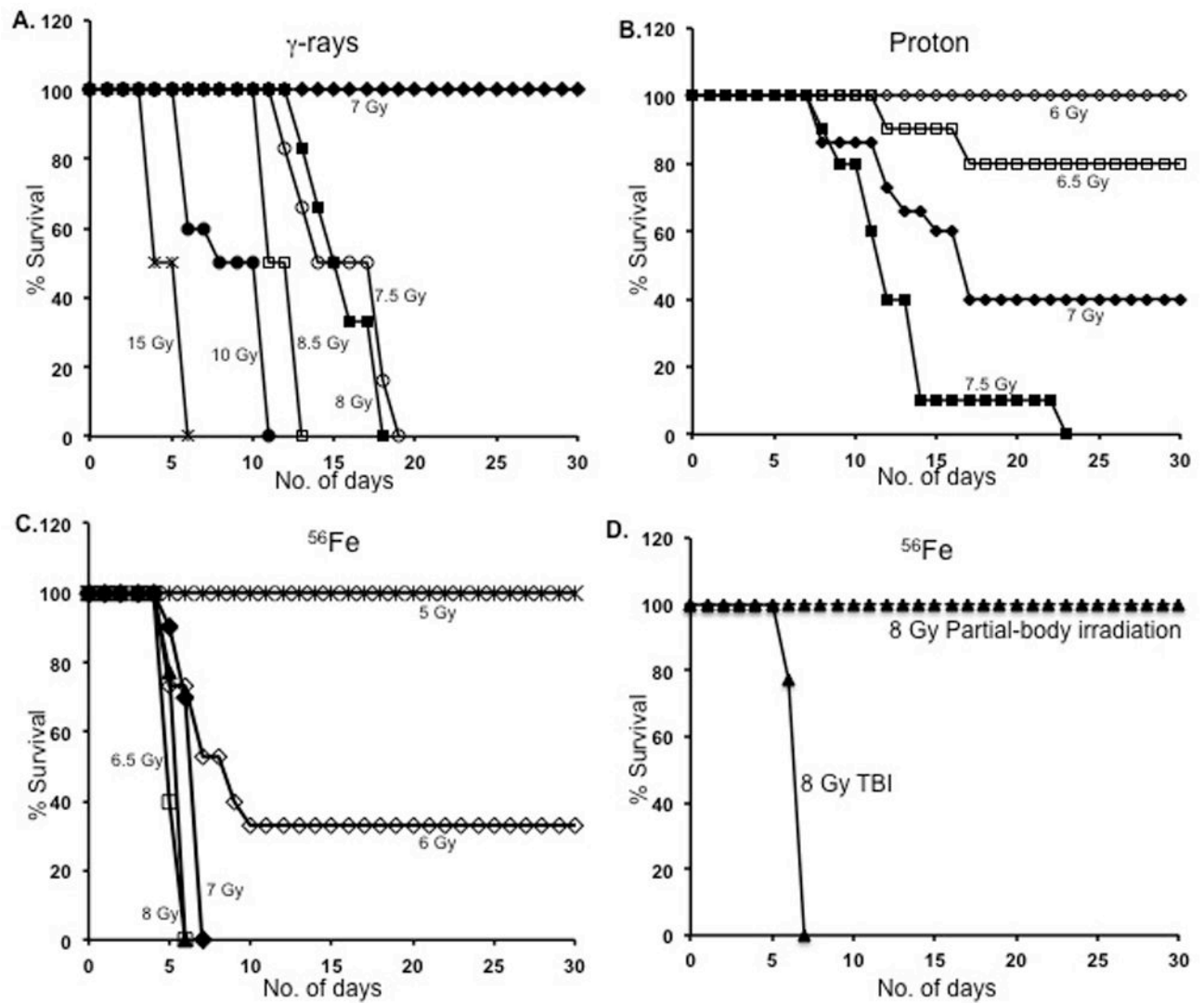


Figure 2.

Time course of lethality for γ -, proton-, and ^{56}Fe -radiation. A) The mortality pattern after γ -radiation is plotted for doses of 7 to 15 Gy. B) Proton radiation-induced lethality pattern is plotted for doses of 6 to 7.5 Gy. C) Iron ion radiation-induced lethality is plotted for doses of 5 to 8 Gy. D) Percent survival after 8 Gy total body ^{56}Fe radiation is compared to that of partial body ^{56}Fe radiation at over 30 d; TBI: Total body irradiation (TBI). For partial body irradiation, the hind limbs were shielded from exposure.

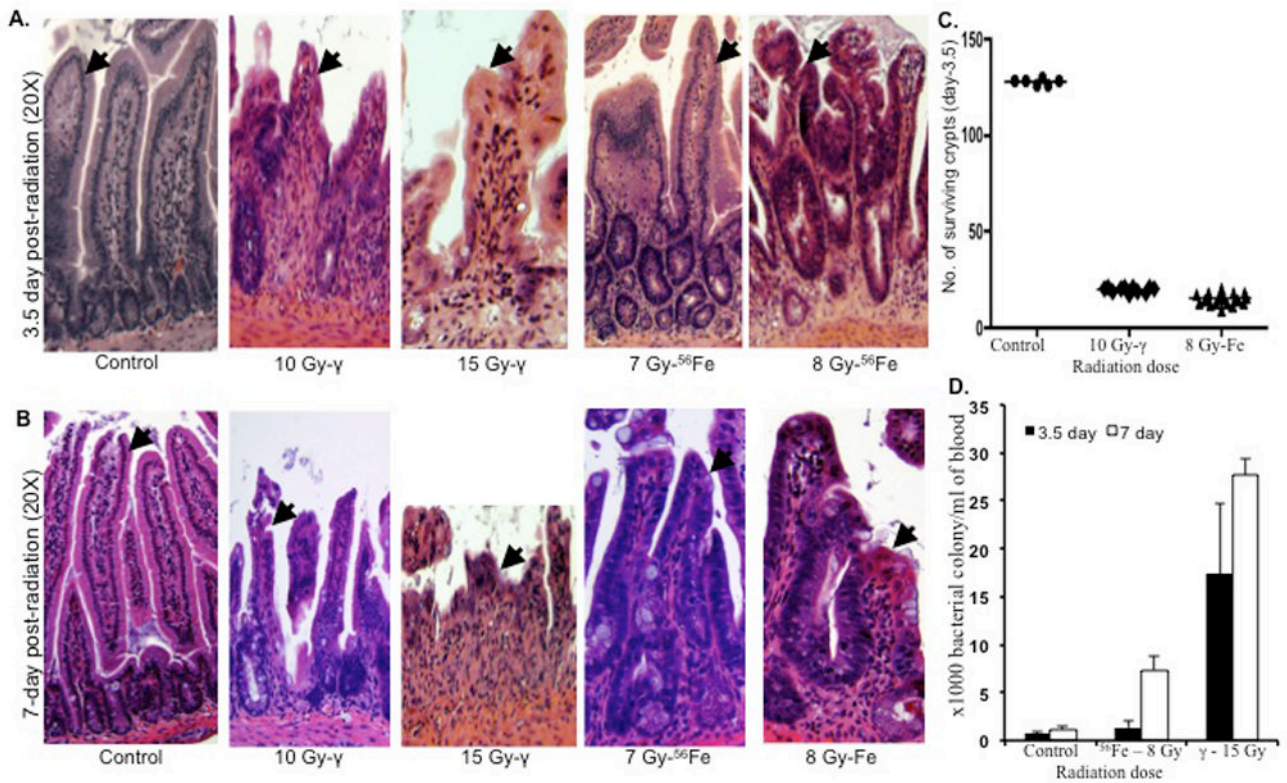


Figure 3.

Intestinal responses in mice (n=3 per group, per time point, and per radiation dose) after ^{56}Fe and γ -radiation. A) H&E stained intestinal histology of jejunal sections at 3.5 d after exposure to γ (10 and 15 Gy) and ^{56}Fe (7 and 8 Gy) radiation. Arrow shows epithelial lining and depicted images are at 20X magnification. B) H&E stained intestinal histology of jejunal sections at 7 d after exposure to γ (10 and 15 Gy) and ^{56}Fe (7 and 8 Gy) radiation. Arrow shows epithelial lining and depicted images are at 20X magnification. C) Number of surviving crypts in jejunal sections at 3.5 d after exposure to 10 Gy of γ and 8 Gy of ^{56}Fe radiation. D) Blood culture at 3.5 d and 7 d after exposure to γ (15 Gy) and ^{56}Fe (8 Gy) radiation. Results are presented as bacterial colonies $\times 10^3$ per ml of blood. * $p < 0.05$ compared to 3.5 d counts for both γ and ^{56}Fe radiation. Error bars represent the standard error of the mean (SEM).

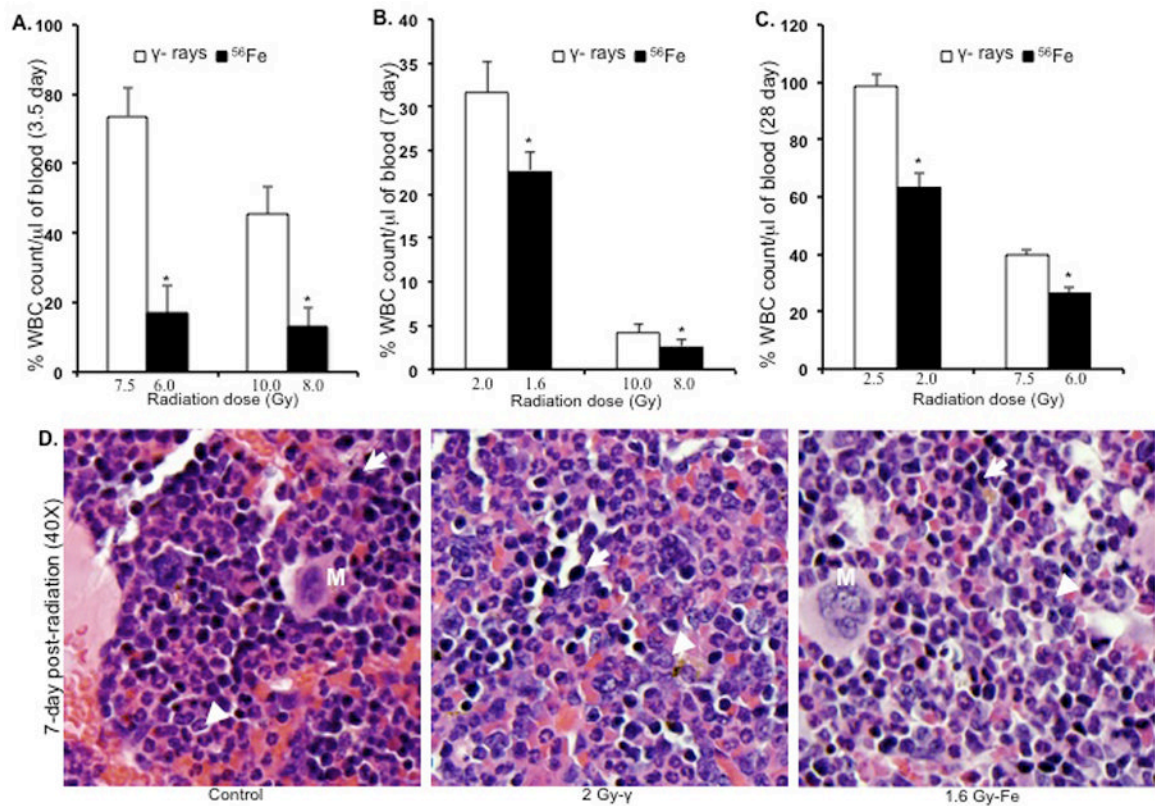


Figure 4.

Peripheral white blood cell (WBC) counts and bone marrow histology (n=3 mice per group, per time point, and per radiation dose). A) WBC counts at 3.5 d after 7.5 and 10 Gy of γ and equitoxic doses (6 and 8 Gy) of ^{56}Fe radiation. * $p < 0.004$ compared to γ radiation. B) WBC counts at 7 d after 2 and 10 Gy of γ and equitoxic doses (1.6 and 8 Gy) of ^{56}Fe radiation. * $p < 0.05$ compared to γ radiation. C) WBC counts at 28 d after 2.5 and 7.5 Gy of γ and equitoxic doses (2 and 6 Gy) of ^{56}Fe radiation. * $P < 0.04$ compared to γ radiation. D) Bone marrow histology at 7 d after 2 Gy and equitoxic dose (1.6 Gy) of ^{56}Fe showing apparent difference in myeloid precursor cell population. Presented images are at 40X magnification. Arrow: erythroid precursor; Arrowhead: myeloid precursor; M: megakaryocyte. Error bars represent the standard error of the mean (SEM).

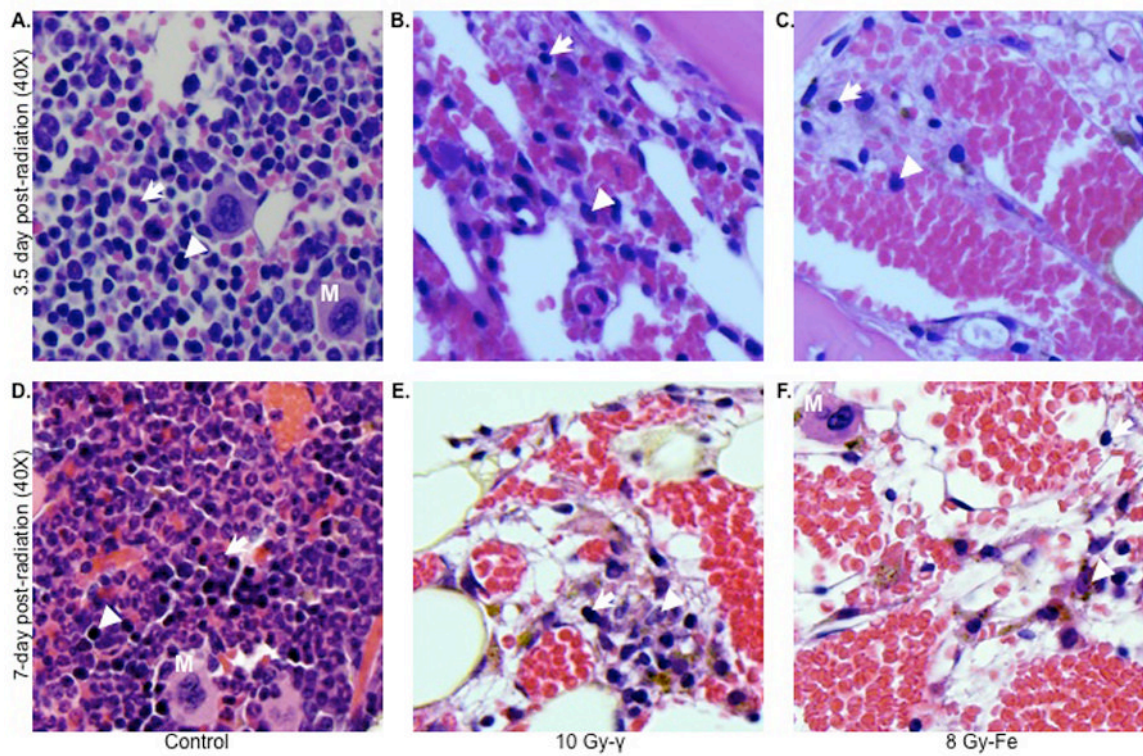


Figure 5. Differential effects of γ and ^{56}Fe radiation on bone marrow cells at lethal doses (n=3 mice per group, per time point, and per radiation dose). Upper panel shows bone marrow sections at 3.5 d after 10 Gy of γ (B) and 8 Gy of ^{56}Fe (C) radiation. Lower panel shows bone marrow sections at 7 d after 10 Gy of γ (E) and 8 Gy of ^{56}Fe (F) radiation. Panels (A) and (D) represent unirradiated control sections. Presented images are at 40X magnification. Arrow: erythroid precursor; Arrowhead: myeloid precursor; M: megakaryocyte.

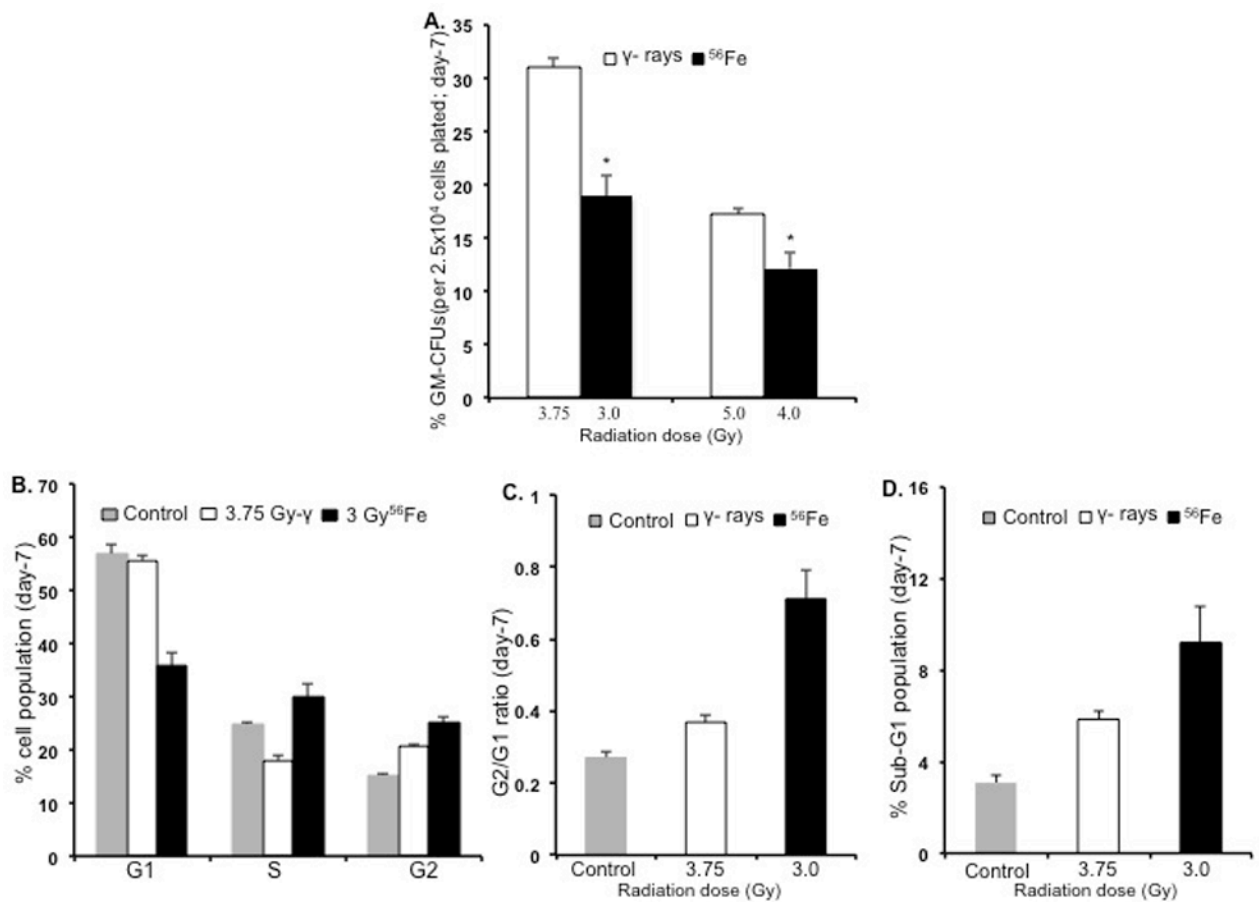


Figure 6.

Bone marrow granulocyte and macrophage colony forming unit (GM-CFU) and cell cycle analysis ($n=3$ mice per group per radiation dose). A) GM-CFU, expressed as percent of control, at 7 d after 3.75 or 5 Gy of γ radiation and respective equitoxic doses (3 or 4 Gy) of ^{56}Fe radiation. $*p<0.04$ compared to γ radiation. B) Bone marrow cell cycle analysis at 7 d after 3.75 Gy of γ radiation and equitoxic dose of ^{56}Fe (3 Gy) radiation; the G2/G1 ratio for the same samples is shown in panel C and the sub-G1 population in panel D. $*p<0.04$ compared to γ radiation. Error bars represent the standard error of the mean (SEM).

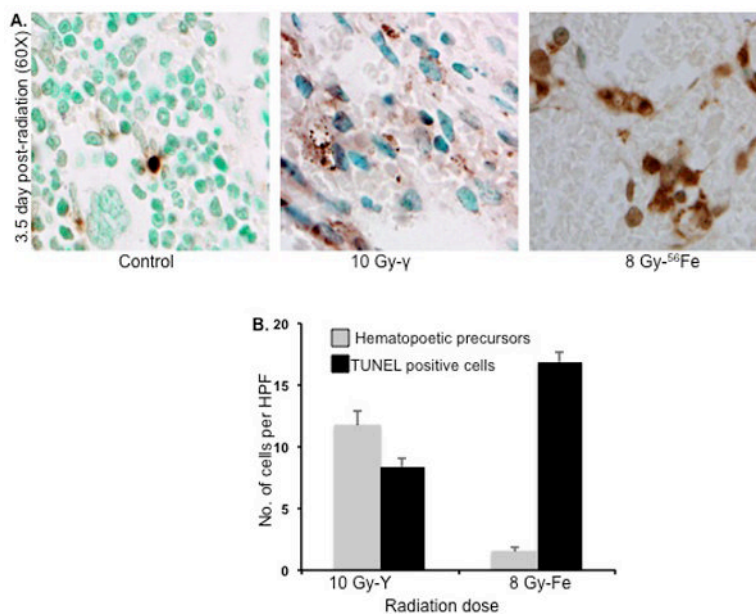


Figure 7. TUNEL staining of bone marrow sections at 3.5 d after irradiation (n=3 mice per group per radiation dose). A) TUNEL stained representative bone marrow sections after γ (10 Gy) and ^{56}Fe (8 Gy) radiation. Presented images are at 60X magnification in oil. B) Quantitative analysis of TUNEL-positive (stained dark brown) and nucleated precursor (counterstained with methyl green) cells after 10 Gy of γ or 8 Gy of ^{56}Fe radiation presented as number of cells per high power field (HPF). * $p < 0.001$ compared to γ radiation counts. Error bars represent the standard error of the mean (SEM).